Methanol oxidation on Ru/Pd(poly) in alkaline solution

S. Štrbac, A. Maksić, Z. Rakočević

PII: S1572-6657(18)30425-9
DOI: doi:10.1016/j.jelechem.2018.06.011
Reference: JEAC 4109

To appear in: *Journal of Electroanalytical Chemistry*

Received date: 7 February 2018
Revised date: 11 May 2018
Accepted date: 5 June 2018

Please cite this article as: S. Štrbac, A. Maksić, Z. Rakočević , Methanol oxidation on Ru/Pd(poly) in alkaline solution. Jeac (2017), doi:10.1016/j.jelechem.2018.06.011

Methanol oxidation on Ru/Pd(poly) in alkaline solution

S.Štrbac[a,*], A.Maksić[b], Z.Rakočević[b],

[a,*]ICTM Institute of Electrochemistry, University of Belgrade, Njegoseva 12, 11001 Belgrade, Serbia

[b]INS Vinca, Laboratory of Atomic Physics, University of Belgrade, Mike Alasa 12–14, 11001 Belgrade, Serbia

Abstract

Polycrystalline Pd electrode, Pd(poly), is modified by Ru nanoislands using spontaneous deposition method. Coverage of Pd(poly) electrode with the deposited Ru are approx. 20, 30 and 50 % as estimated from phase atomic force microscopy images. The oxidation state of Pd substrate and the deposited Ru is determined by X-ray spectroscopy (XPS). Electrocatalytic activity of obtained Ru/Pd(poly) bimetallic electrodes is tested toward methanol oxidation in alkaline medium. Cyclic voltammetry and chronoamperometry experiments show the enhanced activity of Ru/Pd(poly) electrodes toward methanol electrooxidation with respect to bare Pd(poly). This is explained by the presence of Ru islands, which provided RuOH and Pd-RuOH sites, necessary for the oxidation of CO as the main intermediate during the oxidation of methanol at lower potentials. 30% Ru/Pd(poly) is the most active of all examined electrodes.

Key words: ruthenum; palladium; spontaneous deposition; methanol oxidation.

[*]*Corresponding author: E-mail: sstrbac@tmf.bg.ac.rs*

Phone: +381 11 3370 389

1. Introduction

The electrochemical oxidation of methanol is one of the main anodic reactions in fuel cells, as primary electrochemical devices that generate electrical energy by conversion from the chemical energy of fuel oxidation [1]. The oxidation of methanol is a multistep reaction, which involves the adsorption and subsequent dehydrogenation of methanol molecules, electron transfer and product desorption. It might proceed either through carbonate pathway with CO as the main poisoning intermediate, or through formate pathway with formaldehyde as one of the main reaction intermediates [1-3]. The reaction occurs with faster kinetics in an alkaline than in acid medium [3], but the use of methanol as a fuel in alkaline fuel cells was limited due to the carbonation of the solution until the development of anion exchange membranes [4-6]. Besides, the high cost of almost exclusively used Pt directed research towards catalysts with either low-Pt content or towards the other metals [7,8].

Methanol oxidation on Pd-based catalysts in alkaline media has also attracted attention in recent years [9]. Since both carbonate and formate were detected as the reaction products it was assumed that methanol oxidation occurs in parallel through both pathways [10]. In the case of incomplete methanol oxidation, both adsorbed CO and different formyl species may be produced, in which case there is a need to modify Pd catalyst with another metal which would favor their further oxidation. In an early work, where Pd substrate was modified by gold adatoms, bifunctional mechanism for the oxidation of methanol was proposed [11], according to which methanol is adsorbed and dehydrogenated on Pd substrate surface sites, while on Au-Pd sites the adsorbed oxygen species take place in further oxidation of reaction intermediates to CO_2. The role of the second metal, Me, in the proposed bifunctional pathway involving formyl species can be summarizes according to ref. [11]:

$CH_3OH + 4\ Pd_{(subs)} = Pd_{(subs)}\text{-}HCO_{ads} + 3Pd_{(subs)}\text{-}H_{ads}$ (1)

$Pd_{(subs)}\text{-}H_{ads} = Pd_{(subs)} + H^+ + e$ (2)

$Pd_{(subs)}\text{-}HCO_{ads} + Pd_{(subs)}\text{-}Me\text{-}O = CO_2 + H^+ + e + Pd_{(subs)} + Pd_{(subs)}\text{-}Me$ (3)

The promotional effect of the second metal (Au, Ru), which provides oxygen containing species is related to the fact that poisoning species which are adsorbed on palladium substrate surface as reaction intermediates can be further oxidized by their presence in the potential region of methanol oxidation in alkaline medium [11,12].

Similar effect of the second metal was reported for the other bimetallic systems including our recent work, where it was shown that polycrystalline Pt modified by spontaneously deposited Pd nanoislands with submonolayer coverage exhibited enhanced activity for methanol oxidation in alkaline medium [13]. It was proposed that Pd, which in this case would be the second metal, was the one at which oxygen containing (OH^-) species were adsorbed promoting thus further oxidation of adsorbed poisoning species. It was also proposed that methanol oxidation occurs through carbonate pathway with CO as an intermediate adsorbed on free Pt substrate sites:

$CH_3OH + 4\ Pd\text{-}OH^- = Pt_{(subs)}\text{-}CO_{ads} + 4H_2O + 4e$ (4)

$Pd\text{-}OH^- = Pd\text{-}OH_{ads} + e$ (5)

$Pt_{(subs)}\text{-}CO_{ads} + 2Pd\text{-}OH_{ads} + 2OH^- = CO_3^{2-} + 2H_2O$ (6)

In this work, polycrystalline Pd, Pd(poly), was modified by ruthenium nanoislands with submonolayer coverage using spontaneous deposition technique. The obtained bimetallic Ru/Pd(poly) electrodes were characterized *ex situ* by atomic force microscopy (AFM) and X-ray photoelectron spectroscopy (XPS), and *in situ* by cyclic voltammetry in 0.1 M KOH solution. Subsequently, the activity of such bimetallic electrodes was tested for methanol electrooxidation reaction in the same alkaline media using cyclic voltammetry and chronoamperometry techniques.

2. Experimental

2.1. Preparation of Ru/Pd(poly) bimetallic electrode

Ruthenium was deposited spontaneously on polycrystalline palladium electrode (diameter of 5 mm, geometric surface area of 0.196 cm^2) from at least two weeks aged (1 mM $RuCl_3 \cdot aq$ + 0.05 M H_2SO_4). It is reported that Ru complexes, which exist in aged brown colored acid solutions, identified as hydrated ruthenyl, RuO^{2+} or the aqua complex: $[RuO(H_2O)_4]^{2+}$, are solution precursors of the spontaneously deposited ruthenium [14].

Depositing Ru solution was prepared with suprapure H_2SO_4 (Merck) and $RuCl_3 \cdot aq$ (Merck). The deposition was conducted by the immersion of palladium electrode into the depositing solution for 1, 3 and 30 min at the open circuit potential (OCP). As prepared different bimetallic Ru/Pd(poly) electrodes were used for *ex situ* AFM and XPS characterization, and as working electrode for the electrochemical measurements. Before and after each measurement, the electrode was polished electrochemically in non-aqueous solution consisting of 0.5 M LiCl and 0.2 M $Mg(ClO_4)_2$, both dissolved in methanol [14], to remove ruthenium deposit and to ensure the smoothness and cleanliness of the palladium substrate surface. For electrochemical measurement, after preparation the electrodes were rinsed, and their surface protected by a drop of water before being transferred through the air to the electrochemical cell. For *ex situ* AFM and XPS measurements no such protection was possible, therefore a bit of surface oxide or other contaminants might be expected, but not to the extent which would significantly influence the main features of bimetallic electrodes.

2.2. AFM imaging of Ru/Pd(poly)

The main surface properties of the obtained Ru/Pd(poly) electrodes were determined by tapping mode AFM using Multimode Quadrex SPM (Veeco Instruments, Inc.) with a commercial Veeco RFESP AFM probe (Nanoscience instruments, Inc.). Description of the importance for simultaneous recording of the height and phase images for comparison of the surface topography from height images and deposit domains visible from phase images due to the mapping of chemical differences between the deposit and substrate was reported earlier [15,16], including AFM images of polycrystalline palladium electrode, the same one that was used in this study as substrate [16]. Average root mean square surface roughness, RMS, is estimated using Veeco subprogram, and taken as the average value from height AFM images with the sizes of (500 x 500) mm^2 and (1 x 1) nm^2 recorded over different areas of the investigated surface.

2.3. X-ray photoelectron spectroscopy measurements

X-ray photoelectron spectroscopy analysis of Ru/Pd(poly) surfaces was used for the determination of the surface chemical constituents and of their oxidation state. XPS measurements on as prepared bimetallic surfaces were carried out *ex situ* using SPECS System with XP50M X-ray source for Focus 500 and PHOIBOS 100/150 analyzer. AlKα source (1486.74 eV) at a 12.5 kV and 32 mA was used for this study. XPS spectra were obtained at a pressure in the range of 3×10^{-8} - 2×10^{-9} mbar. Survey spectra were recorded from 0 – 1000 eV, with the energy step of 0.1 eV, dwell time of 0.5 s, and with pass energy of 40 eV in the Fixed Analyzer Transmission (FAT) mode. Region spectra were recorded with the energy step of 0.1 eV, dwell time 2s and pass energy of 20 eV in the FAT mode. Spectra were collected by SpecsLab data analysis software and analyzed by CasaXPS software package both supplied by the manufacturer.

2.4. Electrochemical measurements

Electrochemical measurements were carried out using Pine instruments bipotentiostat AFCBP1 and conventional three electrode cell, with Pd(poly) and different Ru/Pd(poly) electrodes as working electrodes, Pt wire as counter electrode and Ag/AgCl, 3M KCl as reference electrodes. All measurements were performed in the base 0.1 M KOH electrolyte, prepared with KOH pellets (max. 0.05 % Na, EMSURE®, Merck) and ultrapure water (Milli-pure, Simplicity® UV system, 18.2 MΩ·cm), and deaerated by purging high purity (99.999 %) N_2 (Messer).

Electrochemical characterization of obtained electrodes was performed by cyclic voltammetry in the base deaerated 0.1 M KOH solution. CO stripping voltammograms were recorded after bubbling high purity CO (Messer) into the 0.1 M KOH solution for 10 minutes while keeping the potential of the working electrode at -0.50 V to ensure CO adsorption and subsequent nitrogen purging for 20 minutes to remove the solution CO. Cyclic voltammograms for formaldehyde and methanol oxidations were recorded in 0.1 M KOH solution containing either 0.4 M formaldehyde or 0.4 M methanol. Chronoamperometry measurements were performed over a prolonged time by holding the potential at -0.20 V. Methanol and formaldehyde were both purchased from Merck.

3. Results and discussion

3.1. OCP changes during spontaneous Ru deposition on Pd(poly)

Chronopotentiometry curves showing the open circuit potential changes after the immersion of Pd(poly) into the base 0.05 M H_2SO_4 solution, as well as into the same solution

containing dissolved depositing Ru are presented in Fig. 1. In the base solution, the OCP value stabilize quickly at 0.593 V. Immediately after the immersion of Pd(poly) electrode into the Ru containing solution, the OCP value rapidly decreases in the first few minutes, indicating that Ru deposition proceeds with a high rate. After that, OCP changes are slowing down gradually reaching a plateau at 0.54 V after about 10 min, without further noticeable change up to 30 min immersion, indicating that Ru deposition has achieved saturation. For Pd(poly) electrode in contact with the depositing Ru solution, according to the ref. [14], it can be assumed that solution $RuO[(H_2O)_4]^{2+}$ anions, the concentration of which increases with solution aging, are firstly adsorbed and dehydrated on the surface of polycrystalline Pd to yield:

$$RuO[(H_2O)_4]^{2+} \rightarrow RuO_{2ads} + 3H_2O + 2H^+, \quad (7)$$

and these Ru^{4+} ions are further reduced to either Ru^{3+} or to Ru^0, which causes the drop of the potential until it stabilizes at a certain OCP value. The analysis of the oxidation state of as deposited Ru islands by XPS will be given below.

3.2. Surface topography and coverage of Pd(poly) electrode surface by the deposited Ru

AFM images for obtained Ru/Pd(poly) electrodes were recorded for all bimetallic surfaces in both height and phase mode in order to get an insight into the surface morphology and surface chemical inhomogeneity. Since in the beginning, Ru deposition proceeds with a high rate, the differences between the deposit obtained after 1 min and 3 min deposition are somewhat uncertain. The main observation is that the number and size of Ru islands, and subsequently the overall surface coverage are higher for larger deposition time of 3 min. Due to the lack of clearly visible difference, the results of AFM analysis will be given for both, but the AFM images will be presented only for 3 min deposition. AFM images recorded at a

saturation Ru deposition, which was certainly achieved after 30 min deposition will also be presented.

Height and phase top-view AFM images of Ru/Pd(poly) surface nanostructures, obtained for 3 and 30 min deposition time are presented in Fig. 2. Surface topography from AFM image, Fig. 1a, reveals that the deposition of Ru occurs on polycrystalline palladium surface which is composed of various clearly distinguished larger crystallites. Although on such an image Ru islands can hardly be distinguished from Pd substrate, they can be recognized on cross-sections as illustrated in Fig. 2b. By drowing the base lines (dotted red lines) bordering the surface of palladium crystallites and Ru deposit, the height of the deposited Ru islands is estimated to be in the range from 0.25 to 1 nm. Similar heigh range is estimated for 1 min deposition. On the other hand, phase AFM images are sensitive to the chemical variations over the surface, meaning that the degree of chemical difference between the substrate and the deposit is proportional to the differences in the z-scale amplitude. Therefore, foreign deposit can be clearly distinguished from the substrate by setting up the treshold to the value below which Pd(poly) surface appear only as (blue) background as presented in Fig. 2c. From such image, the fraction of the overall area other than the background gives the coverage as the percentage of the palladium surface covered by the deposited Ru islands. Coverage of the palladium substrate with deposited Pd islands is estimated to be (30 ± 5)%. Lateral size of Ru islands as determined from the cross section, Fig. 2d, ranged from 5–20 nm, indicating that the deposited islands are partly agglomerated. Similarly, for Ru/Pd(poly) surface obtained after 1 min deposition time, the estimated coverage was (20 ± 5)%, while the lateral island size ranged from 2-10 nm indicating lower degree of agglomeration. For Ru/Pd(poly) surface obtained after 30 min Ru deposition, height AFM image presented in Fig. 2e, shows similar surface topography, while from corresponding cross section, Fig. 2f, it can be seen that the height of the deposited Ru islands

ranged from 0.5 to 2.5 nm. From phase AFM image, Fig. 2g, the estimated coverage was (50 ± 5) %, and from cross section analysis, Fig. 2f, gives that the lateral size ranged from 10-25 nm. These results show the presence of larger Ru islands and higher degree of their agglomeration for the deposition time of 30 min.

Since the amount of the deposited Ru is directly dependent on the deposition rate, which is not constant but slows down with time, no linear dependence of the palladium surface coverage with the deposition time could be expected. Moreover, for the deposition times longer than 10 min, the OCP reaches plateau, indicating that the stationary state (the deposition rate equals the dissolution rate) is achieved, and that the saturation coverage is achieved. Similar was observed for spontaneous Ru deposition on Au(111) and Pt(111), where it was shown that the increase in surface coverage above saturation, which was lower than the full coverage of the electrode, could be achieved only by repetitive deposition method [17,18].

Average RMS roughness, which was reported to be (3.4 ± 0.7) nm for bare Pd(poly) [15], does not change after Ru deposition, and with the estimated values that fall within the range of statistical error for bare Pd(poly), no significant change in the surface area can be observed.

3.3. The oxidation state of Ru/Pd(poly) surface constituents

XPS spectra of 30% Ru/Pd(poly) electrode overlapped with the spectra for bare Pd(poly), which were recorded in order to get a better insight into the oxidation state of the deposited Ru, are presented in Fig. 3. Survey spectra from Fig. 3a show the positions of the main peaks characteristic of the main elements, from which the electrode surface is composed of. These peaks are: Pd 3d, Pd 3p, Ru 3d, O 1s and C 1s, originating from Pd(poly) substrate,

deposited Ru islands, oxygen containing species and carbon containing contaminant, respectively.

Enlarged XPS spectrum of 30% Ru/Pd(poly) electrode overlapped with the spectrum for bare Pd(poly), Fig. 3b, show Pd 3d doublet peaks, characteristic for bare palladium substrate, and Ru 3d doublet peaks, characteristic for bare Ru deposit masked by C 1s peak originating from carbon contaminants, which appear in the binding energy region from 280 – 365 eV. For bare Pd(poly), binding energies of 340.32 eV and 335.05 eV, for Pd $3d_{5/2}$ and Pd $3d_{3/2}$ photoelectron lines, respectively, can be attributed to the metallic Pd [19]. For 30% Ru/Pd(poly), the intensity of the two Pd 3d photoelectron lines decreased while the intensity of C 1s line increased, owing to the deposited Ru. The binding energies of Pd $3d_{5/2}$ and Pd $3d_{3/2}$ photoelectron lines are down shifted for 0.15 eV and 0.10 eV, respectively, compared to their position in the spectrum for bare Pd(poly), although Pd remains in the metallic state. This confirms the electronic effect that is manifested through the impact of the deposited Ru on the electronic state of palladium substrate.

Since Ru 3d photoelectron lines are lower in intesity and overlapped with C 1s line around 285 eV, their high resolution spectra were recorded separately and presented in Fig. 3c, together with high resolution C1s line for bare Pd(poly). The spectrum for Ru/Pd(poly) differ from the one for C1s for bare Pd(poly) by the intensity and by the appearance of the peak at lower binding energies corresponding to Ru 3d. The presence of Ru can be seen after fitting spectra obtained on Ru/Pd(poly) by three photoelectron lines. The one with the highest intensity at 284.6 eV for Ru/Pd(poly) corresponds to C 1s peak for graphite [20], similarly as the one at 284.2 eV for C1s peak for bare Pd(poly) [21]. Ru 3d doublet is fitted to Ru $3d_{5/2}$ and Ru $3d_{3/2}$ lines. Ru $3d_{5/2}$ line, which appears at 281.1 eV is shifted for 1.3 eV from the line for metallic Ru (279.8 eV) [22] and can be assigned to either RuO_2 oxide species [22] or to Ru/RuOx [23]. The other Ru $3d_{3/2}$, line, which appears at 284.3 eV corresponds to both

metallic Ru [20] or Ru/RuOx [24]. According to these results, it can be assumed that Ru deposit consists of a mixure of metallic Ru, and different RuOx species. This is in agreement with previous in situ XPS studies at the open circuit potental of Ru spontaneously deposited on Pt [25], and that is the reason why before the electrochemical measurements the potential was held negative enough to reduce deposited RuOx species to the metallic state.

3.4. Cyclic voltammetry characterization of Ru/Pd(poly) electrodes

Cyclic voltammetry profiles of bare Pd(poly) and of bimetallic Ru/Pd(poly) electrodes recorded in the potential range of -0.7 to 0.2 V in 0.1 M KOH are shown in Fig. 4. Potential limits were chosen to characterize the electrode in the potential region relevant for methanol adsorption and oxidation. At the same time, negative potential limit was chosen high enough to avoid an intense evolution/absorption of hydrogen [26,27], while positive potential limit was chosen to be low enough to avoid the formation of high valence oxides of palladium, which can not be effectively reduced in the backward scan and also to avoid the electrochemical dissolution of palladium at higher potentials [26]. Cyclic voltammogram of bare Pd(poly) electrode is in good agreement with voltammograms obtained in alkaline solutions [15,16]. The main features in the forward scan relevant for the state of the surface during methanol oxidation involve the widening of the double layer starting roughly at the potential of -0.45 V wide and the oxidation peak in the potential interval from -0.33 to 0.2 V. The widening of the double layer might be associated with the preoxidation which involves the adsorption of OH anions on Pd surface, while the main oxidation peak involves Pd-OH_{ads} layer formation up to the potential of approx. 0.03 V, which occurs simultaneously with the further electrode surface oxidation and the formation of palladium (II) oxide (PdO) [15,16], while at higher potentials up to the 0.2 V, PdO formation is most likely accompanied by at

least partial formation of higher valence Pd oxides. In the backward scan, a wide peak centered at -0.2 V corresponds to the reduction of the palladium (II) oxide formed during the forward scan. Comparing voltammograms of Ru/Pd(poly) with the one of bare Pd(poly), it can be seen that the broad peak of palladium oxide formation is increasingly supressed, with the increase of the coverage of the deposited ruthenium, from 20% to 30%, and to 50%. Namely, the deposited Ru nanoislands efficiently block palladium surface active sites, which are required for the Pd-OH_{ads} layer formation in the potential region from -0.33 to 0.03 V [15,16], while at the same time the formation of PdO takes place on the remaining Pd surface sites, as well as the formation of higher valence palladium oxides at higher potentials. This all give as a result the lower intensity of Ru/Pd(poly) reduction peaks compared to the one of bare Pd(poly). Oxide reduction peak potential of -0.2 V for bare Pd(poly) is slightly shifted to the more positve values for Ru/Pd(poly), which pointed out to the influence of the deposited Ru. The presence of Ru-oxide species are not clearly recognizable in CVs, but a brief discussion can be made according to the behavior of bare Ru in alkaline solution [28,29]. The reversible oxide formation on bare Ru starts immediatelly after hydrogen evolution reaction which takes place at approx -0.8 V (vs.Ag/AgCl) [29], which is beyond chosen negative potential limit, meaning that the increase in current at lower potential for Ru/Pd(poly) surfaces corresponds to the overlapping of both hydrogen adsorption/oxidation on Ru/Pd surface sites [30] and reversible oxide formation/reduction of the deposited Ru islands. After that, the reversible oxide formation/reduction of bare Ru is relatively featureless on CVs except broadening of the double layer region up to the potential of -0.1 V. It was suggested that in the potential region of reversible RuOx formation, Ru sites on the oxidized surface based on a ‘sandwich’ type structure with Ru/O/Ru composition exist [31], while recently the formation of RuOH was proposed [32] . At higher potentials, the oxidation current increases with increasing potential which was ascribed to the formation and growth of irreversible

higher valence RuO_2 oxides [28,29]. Taking into account such behavior of bare Ru electrode in alkaline solution, the presence of Ru islands on Pd substrate can hardly contribute in any defined manner to the CVs of bimetalllic Ru/Pd(poly) surfaces, except that partial blocking Pd oxide formation due to the presence of Ru islands is indicated in CVs. Oxygen evolution on bare Ru in alkaline solution begins at approx. 0.3 V, simultaneously with the formation of soluble RuO_4^{2-} and RuO_4 species, which were detected by potential modulated reflectance spectroscopy [28], meaning that Ru dissolution does not have any role in these studies, since it occurs at potentials higher than the chosen positive potential limit of 0.2 V. Due to the lack of CV features that would be characteristic for Ru deposited on Pd substrate, and due to the presence of both Pd and Ru as a mixture in different oxidation states in the potential region of surface oxidation, the electrochemically active surface area (EASA) can not be evaluated from reduction peaks. For the same reason, EASAs calculated from CO stripping (see below) charges, which values are for bimetallic surface very close to the one for bare Pd(poly), only indicates that the number of surface active sites does not change significantly after Ru deposition, just like the overall surface area according to the surface roughness discussed above. Similar behavior has been reported for Rh spontaneously deposited on the same Pd(poly) electrode, where for the same coverages of Pd(poly) with Rh islands almost the same effect can be seen on corresponding CV curves, as well as on CO stripping charges [16,27].

3.5. Electrocatalytic activity of Ru/Pd(poly) electrodes for the oxidation of intermediates during different methanol oxidation reaction pathways

3.5.1. CO stripping on Ru/Pd(poly)

In the process of methanol electrooxidation carbon-monoxide appears as an intermediate in carbonate reaction pathway. CO molecules are strongly adsorbed on the

electrode surface thereby blocking the active surface sites and thus preventing the adsorption and subsequent oxidation of methanol molecules. In order to determine the mechanism of methanol electrooxidation reaction, testing the activities of the modified Ru/Pd(poly) electrodes for a further CO oxidation is of the utmost importance. CO stripping curves from Pd(poly) electrode as well as from the ones modified with 20, 30 and 50% Ru are shown in Fig. 5. CO stripping curve from bare Pd(poly) electrode exhibits a broad pre-peak in the Doha,s preoxidation potential region, and one main peak centered at - 0.165 V in the potential region for the main peak for $PdOH_{ads}$ formation (see Fig. 4). The first one refers to the oxidation of weakly adsorbed CO, while the second one refers to the oxidation of strongly adsorbed CO [33]. On the other hand, CO stripping curve for bare Ru in alkaline solution shows a broad peak in the potential region from -0.33 to -0.02 V centered at -0.22 V (vs. Ag/AgCl) [34].

CO stripping curves from bimetallic Ru/Pd(poly) electrodes show that the CO oxidation which would take place in the palladium peroxidation potential region up to -0.27 V is suppressed due to the presence of the deposited Ru and occurs only on the remaining $PdOH_{ads}$ sites. Similarly, CO oxidation taking place on bimetallic surfaces at potentials higher than -0.2 V, up to its end at -0.07 V, i.e., the potential region of the main CO oxidation peak for bare Pd(poly), corresponds to the reaction on the remaining palladium surface sites not covered by the deposited Ru, but oxidized to PdOH. The shift of the peak potentials for CO oxidation from -0.17 V on bare Pd(poly), to the potential of -0.14 V, which corresponds to CO oxidation on remaining PdOH surface sites on Ru/Pd(poly) bimetallic surfaces, is most likely caused by the electronic effect as indicated by the down shift of Pd 3d binding energies due to the presence of Ru. It was reported earlier that alloying platinum with ruthenium lowered platinum 5d bend which led to the weakening of Pt-CO bond and enabled easier electrooxidation of carbon monoxide [28,35-37].

The main CO oxidation peak of modified Ru/Pd(poly) electrodes is located in the potential region from -0.27 V to -0.2 V, and in all cases consists of two overlapped peaks with centers at different potential values. The separation of the CO oxidation peak is due to the difference in the CO binding energy at different surface active sites, i.e. Pd-RuOH edges or bare RuOH sites. The first peak appearing at approx. -0.27 V for all Ru/Pd(poly) electrodes, but with the highest intensity on 30% Ru coverage most likely corresponds to CO oxidation on the edges of Pd-Ru as the most active surface sites for Pd-RuOH formation, which further participate as a reactant during CO oxidation. Accordingly, CO oxidation on RuOH sites takes place in the potential range from -0.22 V to -0.24 V depending on the Ru coverage. It has been shown that CO oxidation on various RuPt and RuPd bimetallic surfaces occurs at different potentials and with different current densities depending on the activity of various surface sites including bare substrate (Pt, Ru) and bare deposit (Pd, Ru) surface sites as well as the Ru-Pt or Ru-Pd edges, or RuPt and RuPd carbon supported nanoparticles [38-40].

CO stripping charges were calculated for the estimation of the electrochemically active surface area (EASA) of obtained bimetallic surfaces, taking into account that the charge for a full CO monolayer adsorbed on bare Pd(poly) substrate was 424 μC cm^{-2} [25]. Approximately, the same value can be used for CO adsorbed on RuPd edge sites or on top of the deposited Ru islands since interatomic distances for Pd ((0.277 nm in Pd(111) and Ru (0.271 nm in Ru(0001)) are close enough. The obtained values for bimetallic 20, 30, and 50% Ru/Pd(poly) surfaces were: 425, 452, and 450 μC cm^{-2}, respectively. This gives that the EASA for 20% Ru/Pd(poly) was 0.197 cm^2, close to the geometric area of 0.196 cm^2 for Pd substrate, while for 30 and 50% Ru/Pd(poly) surfaces the EASAs were 0.209 and 0.205 cm^2, respectively. All current densities in the results presented below were given with respect to the EASA.

3.5.2. Formaldehyde oxidation on Ru/Pd(poly)

The activity of Ru/Pd(poly) with respect to bare Pd(poly) towards formaldehyde as a possible intermediate during methanol oxidation through formate reaction pathway can be tested through its oxidation on respected electrodes as shown on CV curves in Fig. 6. On bare Pd(poly), formaldehyde oxidation reaction starts at -0.4 V, and occurs with a very low current density up to -0.35 V, after which it sharply increases reaching a maximum current density of 8.86 mA cm^{-2} at -0.11 V. A slow gradual decrease of the current density up to the positive potential limit as well as in the backward scan is observed. Formaldehyde oxidation on examined Ru/Pd(poly) electrodes occur in a similar manner, starting at almost the same potential and proceeding with equal intensity up to the very positive potentials, which indicates similar activity of both PdOx and RuOx for formaldehyde oxidation. At higher potentials, current densities increase on bimetallic surfaces achieving the maximum values at potentials which are 40-50 mV more positive than for bare Pd(poly), and not particularly sensitive to the Ru coverage. As will be shown below, the potential region of the enhanced formaldehyde oxidation is not relevant for methanol oxidation.

3.6. Methanol oxidation on Ru/Pd(poly) electrodes

The methanol electrooxidation reaction activity of different Ru/Pd(poly) surfaces compared to the activity of bare Pd(poly) in alkaline solution is presented in Fig. 7. Methanol oxidation on palladium takes place in the potential region from -0.32 V up to 0.09 V. The reaction proceeds quite slowly up to the potential of around -0.16 V, which coincides with a high activity for formaldehyde oxidation (see Fig. 6). With increasing potential, a rapid increase in current density is observed achieving a maximum of 3.28 mA cm^{-2} at approx. -0.12 V. The potential region of a high methanol oxidation reaction rate coincides with a high

palladium activity for CO oxidation (see Fig. 5). In the reverse scan, with cathodic polarization of the electrode, electrooxidation reaction takes place from -0.1 to -0.4 V, and with the lower current density maximum of 1.62 mA cm^{-2} coinciding with a high activity of palladium for formaldehyde oxidation. Methanol oxidation is blocked at higher potentials similarly like formaldehyde oxidation, most likely due to the presence of not active higher valence PdOx surface sites and/or due to the presence of reaction intermediates formed during anodic electrode polarization. Accordingly, lower current density for methanol oxidation at lower potentials is most likely caused by the presence of reaction intermediates formed in the forward scan (coinciding with the activity for formaldehyde oxidation, Fig. 6). Methanol oxidation curves on different Ru/Pd(poly) nanostructures show that in all cases, reaction begins at approximately the same potential of -0.32 V as on bare Pd(poly) electrode (see insert in Fig. 7), and that the oxidation current densities show two maxima. At lower potentials, the first methanol oxidation peak for bimetallic Ru/Pd(poly) show considerably more rapid current density increase with increasing potential compared to bare Pd(poly). Among three examined surfaces the one with 30% Ru coverage has shown the highest activity, with maximum current density of 3.05 mA cm^{-2}, achieved at the potential of -0.16 V. At higher potentials, the second methanol oxidation peak for bimetallic Ru/Pd(poly) surfaces coincides with the peak for methanol oxidation on bare Pd. While for 20% and 30% Ru coverage, methanol oxidation current densities of 3.28 mA cm^{-2}, are comparable to those for bare Pd(poly), for 50% Ru coverage it is significantly lower. Besides, the peak potential of -0.12 V is the lowest for 30% Ru/Pd(poly). So it can be said that 30% Ru/Pd(poly) surface is the most active one for methanol oxidation in alkaline solution, although the activity of 20% Ru/Pd(poly) is close enough to fall in the range of the experimental fluctuations. In the backward scan, the methanol oxidation is blocked at higher potentials on all bimetallic surfaces similarly like on bare palladium, either due to the presence of not active higher

valence PdOx and RuOx surface sites and/or due to the presence of reaction intermediates formed in the forward scan. At lower potentials, methanol oxidation proceeds with lower current density than in the forward scan (coinciding with the potential region for CO oxidation activity, Fig. 5), which is again most likely caused by the presence of reaction intermediates.

The catalytic effect caused by the presence of Ru islands on palladium surface on methanol oxidation with respect to both carbonate and formate reaction pathways will be discussed for the most active 30% Ru/Pd(poly) taking into account its activity towards CO and formaldehyde oxidation as possible reaction intermediates. For comparison, the anodic parts of CVs for methanol oxidation and for the oxidation of their respective intermediates for both Ru modified and bare Pd(poly) electrodes are presented in Fig. 8.

CVs for methanol oxidation, Fig. 8a, CO stripping, Fig. 8b, and formaldehyde oxidation, Fig. 8c, on 30% Ru/Pd(poly) show that the oxidation of these three molecules occurs within practically the same potential region. This means that the oxidation of methanol takes place via so called dual mechanism through both carbonate and formate pathways.

Taking into account that Ru alone is active for methanol oxidation in the potential region from -0.73 to -0.68 V (vs. Ag/AgCl) and inhibited at higher potentials [39], it is supposed that the reaction which is recorded on bimetallic Ru/Pd(poly) at much more positive potentials takes place either on Pd-Ru edges and/or on remaining palladium surface sites, not covered with the deposited Ru. The enhanced activity of 30% Ru/Pd(poly) bimetallic electrode for methanol oxidation at lower potentials, between -0.23 V and -0.35 V, Fig. 8a, coincides with the enhanced activity of the same bimetallic surface for CO oxidation, Fig. 8b. This means that the deposited ruthenium islands obviously facilitate the oxidation of adsorbed reaction CO providing Pd-RuOH surface sites, favoring thus the bi-functional mechanism of methanol oxidation [40,41], in which palladium provides sites for dissociative adsorption of

methanol while ruthenium provides OH, which accelerate methanol electrooxidation reaction [35,36]. The second peak for methanol oxidation on bimetallic 30% Ru/Pd(poly) coincides with the activity of the electrode towards formaldehyde oxidation, which as discussed above might take place on both RuOx and PdOx sites. Therefore it can be assumed that methanol oxidation occurs primarily through formate pathway at higher potentials, and only to the lower extent through CO as an intermediate.

3.7. Chronoamperometry activity and stability test of 30% Ru/Pd(poly) electrode

Stability and activity as well as the poisoning susceptibility of the bimetallic 30% Ru/Pd(poly) compared with bare Pd(poly) electrodes for methanol oxidation were investigated by chronoamperometry. Measurements were performed by keeping the electrodes at a constant potential of -0.2 V for 40 minutes in 0.1 M KOH solution containing 0.4 M methanol. Chronoamperometry curves, recorded by measuring the current density changes over time are shown in Fig. 9. After the initial sharp current densities rise due to the beginning of methanol electrooxidation reaction, current densities drop sharply in the first minutes, than stabilize and show significantly slower decline. Current density decrease at the electrodes in the first few minutes is a result of the electrode surface blocking with accumulated reaction intermediates like adsorbed CO during the reaction. Bimetallic 30% Ru/Pd(poly) electrode has shown better activity over time due to better tolerance to poisoning of the electrode surface by carbon monoxide than bare Pd(poly).

Promotional effect of Ru on the catalytic activity of carbon supported Pd nanoparticles for methanol oxidation in alkaline solution has been studied only recently [12,42-44], where bimetallic RuPd nanoparticles were synthetized using different methods. In contrast to different RuPd/C systems, in this work Ru nanoislands were spontaneously deposited on solid

Pd(poly) substrate with various Ru coverage in order to establish the exact Ru:Pd ratio on the bimetallic electrode surface for which the promotional effect of Ru on the catalytic activity of bare Pd for methanol oxidation in alkaline media would be the highest. Such RuPd system was not studied so far for methanol oxidation, although the activity of bimetallic Pd/Pt(poly) [13] and Rh/Pd(poly) [16] systems prepared in similar way, were explored in our previous work for the studies of methanol and ethanol oxidation, respectively.

Comparison of the activity of Ru/Pd(poly) electrodes with RuPd/C systems can be made by taking into account the relative content of both metals presented as the percentage of Pd surface covered with Ru, or the surface coverage in the case of Ru/Pd(poly) electrodes, and a percentage of Ru and Pd content in RuPd/C nanoparticles. Mass loading ratio of Ru:Pd=1:1 in refs.[12,42], while the one in ref.[43] with Ru:Pd=1:3 ratio have shown the highest activity for methanol oxidation. In this case 50% Ru/Pd(poly), which corresponds to 1:1 surface content ratio has shown the lowest activity, while 30% Ru/Pd(poly) corresponding to 1:2 Ru:Pd surface content ratio has shown the best activity for methanol oxidation.

We believe that the results presented in this work contribute to the understanding of the promotional effect of the presence of Ru with defined surface coverage to the enhancement of the catalytic activity of bare Pd, and consequently to the design of RuPd nanoparticles with the surface Ru:Pd ratio 1:2, which would exhibit the highest activity of such bimetallic electrodes for methanol oxidation in alkaline media.

4. Conclusions

The obtained results have shown that the addition of submonolayer amounts of Ru by spontaneous deposition contributes significantly to the enhancement of the electrocatalytic

activity of Pd electrode towards the oxidation of methanol in alkaline media. Among different bimetallic Ru/Pd(poly) electrodes with respect to the deposit coverage, the one with 30% Ru coverage has shown the highest activity for methanol oxidation. The promoting effect of Ru as the second metal added to bare Pd(poly) has been explained by the presence of Pd-RuOH which promoted the oxidation of CO as the main intermediate during the oxidation of methanol. Besides, the electronic effect between the deposited Ru and Pd(poly) substrate also contributed to the increase of the activity of Ru/Pd(poly) bimetallic surface towards methanol oxidation in alkaline medium.

Acknowledgement:

This work was financially supported by the Ministry of Education, Science and Technological Development of Republic Serbia, project N^{o} III-45005.

References

1. C. Lamy, J.-M. Léger, S. Srinivasan, Direct methanol fuel cells – From a 20th century electrochemist's dream to a 21st century emerging technology, in: J.O'M. Bockris (Ed), Modern Aspects of Electrochemistry, Vol. 34 (Plenum, New York, 2001), Chapter 3, pp. 68-123.

2. E. Hao Yu, K. Scott, R.W. Reeve, A study of the anodic oxidation of methanol on Pt in alkaline solutions, J. Electroanal.Chem. 547 (2003) 17-24.

3. M. Jing, L. Jiang, B. Yi, G. Sun, Comparative study of methanol adsorption and electro-oxidation on carbon-supported platinum in acidic and alkaline electrolytes, J. Electroanal. Chem. 688 (2013) 172-179.

4. K. Matsuoka, Y. Iriyama, T. Abe, M. Matsuoka, Z. Ogumi, Electro-oxidation of methanol and ethylene glycol on platinum in alkaline solution: Poisoning effects and product analysis, Electrochim. Acta 51 (2005) 1085-1090.

5. R. Manoharan, J. Prabhuram, Possibilities of formation of poisoning species on direct methanol fuel cell anodes, J. Power Sources 96 (2001) 220-225.

6. M. Carmo, G. Doubek, R.C. Sekol, M. Linardi, A.D. Taylor, Development and electrochemical studies of membrane electrode assemblies for polymer electrolyte alkaline fuel cells using FAA membrane and ionomer, J. Power Source 230 (2013) 169.

7. H. Liu, C. Song, L. Zhang, J. Zhang, H. Wang, D.P. Wilkinson, A review of anode catalysis in the direct methanol fuel cell, J. Power Source 155 (2006) 95-110.

8. A. Brouzgou, S.Q. Song, P. Tsiakaras, Low and non-platinum electrocatalysts for PEMFCs: current status, challenges and prospects, Appl. Catal. B: Environ. 127 (2012) 371.

9. C. Bianchini, P.K. Shen, Palladium-based electrocatalysts for alcohol oxidation in half cells and in direct alcohol fuel cells, Chem. Rev. 109 (2009) 4183–4206.

10. V. Bambagionni, C. Bianchini, A. Marchionni, J. Philippi, F. Vizza, J. Tedd, P. Serp, M. Zhiani, Pd and Pt–Ru anode electrocatalysts supported on multi-walled carbon nanotubes and their use in passive and active direct alcohol fuel cells with an anion-exchange membrane (alcohol =methanol, ethanol, glycerol), J. Power Sources 190 (2009) 241-251.

11. M. Watanabe, S. Motoo, Electrocatalysis by ad-atoms. Part I. Enhancement of the oxidation of methanol on platinum and palladium by gold ad-atoms J. Electroanal. Chem. 60 (1975) 259- 266.

12. Y. Chen, L. Zhuang, J. Lu, Non-Pt Anode Catalysts for Alkaline Direct Alcohol Fuel Cells, Chin. J. Catal. 28 (2007) 870-874.

13. A. Maksić, Z. Rakočević, M. Smiljanić, M. Nenadović, S. Štrbac, Methanol oxidation on Pd/Pt(poly) in alkaline solution, J. Power Sources 273 (2015) 724–734.

14. W. Chrzanowski, H. Kim and A. Wieckowski, Enhancement in methanol oxidation by spontaneously deposited ruthenium on low-index platinum electrodes, Catal. Lett. 50 (1998) 69-75.

15. I. Srejić, Z. Rakočević, M. Nenadović, S. Štrbac, Oxygen reduction on polycrystalline palladium in acid and alkaline solutions: topographical and chemical Pd surface changes, Electrochim. Acta 169 (2015) 22–31.

16. A. Maksić, M.Smiljanić, Š. Miljanić, Z. Rakočević, S. Štrbac, Ethanol oxidation on Rh/Pd(poly) in alkaline solution, Electrochim. Acta 209 (2016) 323-331.

17. S. Štrbac, R. J. Behm, A. Crown, A. Wieckowski, In situ STM imaging of spontaneously deposited ruthenium on Au(111) Surf. Sci. 517 (2002) 207–218.

18. S. Štrbac, C. M. Johnston, G. Q. Lu, A. Crown, A. Wieckowski, In situ STM study of nanosized Ru and Os islands spontaneously deposited on Pt(111) and Au(111) electrodes, Surf. Sci. 573 (2004) 80–99.

19. C.J. Jenks, S.L. Chang, J.W. Anderegg, P.A. Thiel, D.W. Lynch, Photoelectron spectra of an Al70Pd 21Mn9 quasicrystal and the cubic alloy Al60Pd25Mn15, Phys. Rev. B: Condens. Matter, 54, (1996) 6301–6303.

20. Y. Xie, P.M.A. Sherwood, Ultrahigh purity graphite electrode by core level and valence band XPS, Surf. Sci. Spectra, 1 (1992) 367-372.

21. F. Arezzo, E. Severini, N. Zacchetti, An XPS study of diamond films grown on differently pretreated silicon substrates, Surf. Interface Anal. 22 (1994) 218-223.

22. D.J. Morgan, Resolving ruthenium: XPS studies of common ruthenium materials, Surf. Interface Anal. 47 (2015) 1072-1079.

23. A.J. McEvoy, W. Gissler, ESCA spectra and electronic properties of some ruthenium compounds, Phys. Status Solidi A, 69 (1982) K91-K96.

24. J.Y. Shen, A. Adnot, S. Kaliaguine, An ESCA study of the interaction of oxygen with the surface of ruthenium, Appl. Surf. Sci. 51 (1991) 47-60.

25. H. Kim, I. Rabelo de Moraes, G. Tremiliosi-Filho, R. Haasch, A. Wieckowski, Chemical state of Ru submonolayers on a Pt(111) electrode, Surf. Sci. (2001) L203-L212.

26. M. Grden, M. Łukaszewski, G. Jerkiewicz, A. Czerwinski, Electrochemical behaviour of palladium electrode: Oxidation, electrodissolution and ionic adsorption, Electrochim. Acta 53 (2008) 7583–7598.

27. S. Štrbac, M. Smiljanić, Z. Rakočević, Electrocatalysis of hydrogen evolution on polycrystalline palladium by rhodium nanoislands in alkaline solution, J. Electroanal. Chem. 755 (2015) 115–121.

28. R.C. Walker, M. Bailes, L.M. Peter, A study of the anodic behaviour of ruthenium by potential modulated reflectance spectroscopy, Electrochim. Acta 44 (1998) 1289-1294.

29. J. Prakash, H. Joachin, Electrocatalytic activity of ruthenium for oxygen reduction in alkaline solution, Electrochim. Acta 45 (2000) 2289–2296.

30. S. St. John, R.W. Atkinson, R.R. Unocic, T.A. Zawodzinski, Jr., A.B. Papandrew, Ruthenium-alloy electrocatalysts with tunable hydrogen oxidation kinetics in alkaline electrolyte, J. Phys. Chem. C, 119 (2015), 13481-13487.

31. N. A. Anastasijevic, Z.M. Dimitrijevic, R.R. Adzic, Oxygen reduction on ruthenium electrode in alkaline electrolytes, J. Electroanal. Chem. 199 (1986) 351-364.

32. T.P. Moffat, M. Walker, P.J. Chen, J.E. Bonevich, W.F. Egelhoff, L. Richter, C. Witt, T. Aaltonen, M. Ritala, M. Leskelä, D. Josella, Electrodeposition of Cu on Ru barrier layers for damascene processing, J.Elecrochem.Soc. 153 (2006) 37-50.

33. K. Nishimura, K. Kunimatsu, M. Enyo, Electrocatalysis on Pd + Au alloy electrodes-Part III. IR spectroscopic studies on the surface species derived from CO and CHOH in NaOH solution, J. Electroanal. Chem. 260 (1989) 167-179.

34. C. Grimmer, R. Zacharias, M. Grandi, B. Cermenek, A. Schenk, S. Weinberger, F-A. Mautner, B. Bitschnau, V. Hacker, Carbon supported ruthenium as anode catalyst for alkaline direct borohydride fuel cells, J. Phys. Chem. C 119 (2015) 23839-23844.

35. P. Liu, J.K. Nørskov, Kinetics of the anode processes in PEM fuel cells - The promoting effect of Ru in PtRu anodes, Fuel Cells 1 (2001) 192-201.

36. W. Sugimoto, K. Aoyama, T. Kawaguchi, Y. Murakami, Y. Takasu, Kinetics of CH_3OH oxidation on PtRu/C studied by impedance and CO stripping voltammetry, J. Electroanal. Chem. 576 (2005) 215–221.

37. H. Hartmann, T. Diemant, J. Bansmann, R.J. Behm, Chemical properties of structurally well-defined PdRu/Ru(0001) surface alloys –Interaction with CO, Surf. Sci. 603 (2009) 1456–1466.

38. J.S. Spendelow, G.Q. Lu, P.J.A. Kenis, A. Wieckowski, Electrooxidation of adsorbed CO on Pt(111) and Pt(111)/Ru in alkaline media and comparison with results from acidic media, J. Electroanal. Chem. 568 (2004) 215–224.

39. J.M. Fisher, N. Cabello-Moreno, E. Christian, D. Thompsett, Methanol oxidation activity of PdRu alloy nanoparticles in direct methanol fuel cells, Electrochem. Solid-State Lett. 12 (2009) B77-B81.

40. F.J. Scott, C. Roth, D.E. Ramaker, Kinetics of CO poisoning in simulated reformate and effect of Ru island morphology on PtRu fuel cell catalysts as determined by operando X-ray absorption near edge spectroscopy, J. Phys. Chem. C 111 (2007) 11403-11413.

41. T. Frelink, W. Visscher, J.A.R. van Veen, Measurement of the Ru surface content of electrocodeposited PtRu electrodes with the electrochemical quartz crystal microbalance: Implications for methanol and CO electrooxidation, Langmuir 12 (1996) 3702-3708.

42. H. Xu, B. Yan, K. Zhang, J. Wang, S. Li, C. Wang, Y. Shiraishi, Y. Dua, P. Yang, Facile fabrication of novel PdRu nanoflowers as highly active catalysts for the electrooxidation of methanol, J. Colloid Interf. Sci. 505 (2017) 1-8.

43. T. Jurzinski, P. Kammerer, C. Cremers, K. Pinkwart, J. Tübke, Investigation of ruthenium promoted palladium catalysts for methanol electrooxidation in alkaline media, J. Power Sources 303 (2016) 182-193.

44. M. Kübler, T. Jurzinsky, D. Ziegenbalg, C. Cremers, Methanol oxidation reaction on core-shell structured Ruthenium-Palladium nanoparticles: Relationship between structure and electrochemical behavior, J. Power Sources 375 (2018) 320-334.

Figure Captions

Fig. 1. Chronopotentiometry curves showing the OCPs changes after immersion of Pd(poly) electrode into depositing (1 mM $RuCl_3 \cdot aq$ + 0.05 M H_2SO_4) solution, compared to the OCP of Pd(poly) immersed into the base electrolyte.

Fig. 2. AFM images (500 x 500) nm^2 of Ru/Pd(poly) obtained after 3 min (left column) and after 30 min (right column) Ru deposition: a) height image after 3 min Ru deposition, z-range 31.8 nm; b) cross-section along the line indicated in the height image, dotted lines show the border between Pd substrate below and Ru deposit above; c) phase image recorded with z-range of 3.2^o, and presented for the phase lag of 0.3^o; d) corresponding cross-section; e) and f) height image after 30 min deposition, z-range 41.5 nm and cross-section; g) and e) phase image, z-range 4.2^o, phase lag 0^o, and cross-section.

Fig. 3. XPS spectra taken from bare Pd(poly) and 30% Ru/Pd(poly): a) survey showing the positions of the main components; b) high resolution spectra showing the binding energies of Pd 3d photoelectron lines and of Ru 3d lines overlapped with C 1s; c) region spectrum showing the fitted binding energies of C 1s and Ru 3d lines.

Fig. 4. CV profiles of bare Pd(poly), and of Ru/Pd(poly) electrodes recorded in 0.1 M KOH at a scan rate of 50 mV/s. Current densities are referred to geometric surface area.

Fig. 5. CO stripping from Pd(poly) and from Ru/Pd(poly) surfaces in 0.1 M KOH. CV curves were recorded at a scan rate of 50 mV/s. Current densities are referred to geometric surface area.

Fig. 6. Oxidation of formaldehyde on Pd(poly) and on Ru/Pd(poly). CV curves were recorded at a scan rate of 50 mV/s in (0.4 M formaldehyde + 0.1 M NaOH) solution. Current densities are referred to EASA.

Fig. 7. The activity of Ru/Pd(poly) compared to Pd(poly) for methanol oxidation in (0.4 M CH_3OH + 0.1 M KOH). CV curves were recorded at a scan rate of 50 mV/s. Current densities are referred to EASA.

Fig. 8. Comparison of the electrocatalytic activity of 30% Ru/Pd(poly) with the activity of bare Pd(poly) for the oxidation of methanol and its possible reaction intermediates: a) methanol oxidation; b) CO stripping; c) formaldehyde oxidation. Current densities are referred to EASA.

Fig. 9. Chronoamperometry measurements of the electrocatalytic activity of 30% Ru/Pd(poly) and Pd(poly) in 0.1 M KOH for the oxidation of methanol. Current densities are referred to EASA.

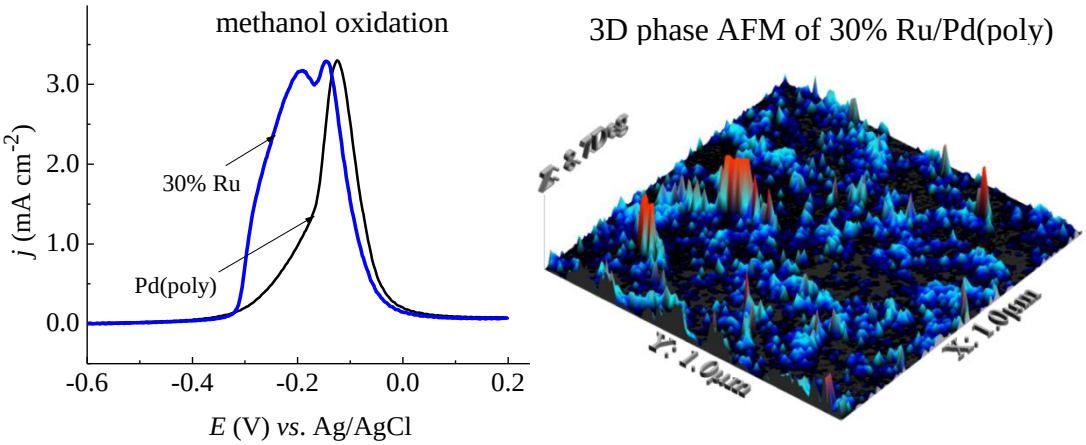

Graphical abstract

Highlights

- Ru nanoislands are deposited spontaneously on Pd(poly) at submonolayer coverage.
- Ru/Pd(poly) nanostructures are characterized by AFM and XPS.
- Methanol oxidation in alkaline media is promoted by the addition of Ru.
- Ru islands provided Pd-RuOH which facilitated the oxidation of CO intermediate.

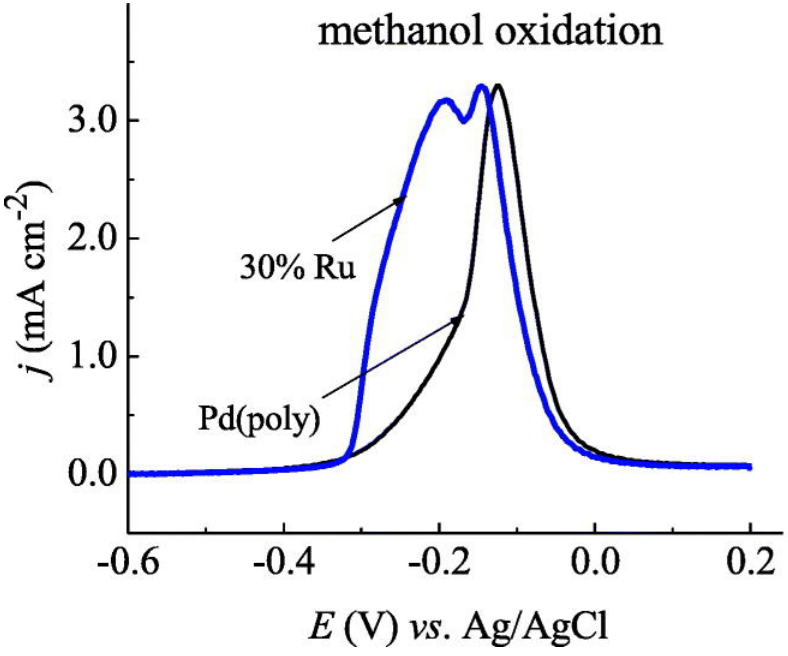

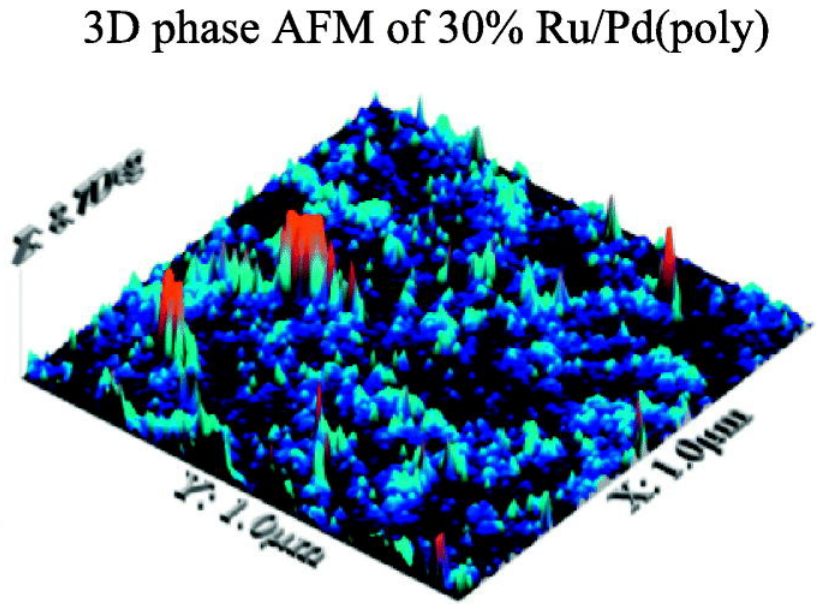

Graphics Abstract

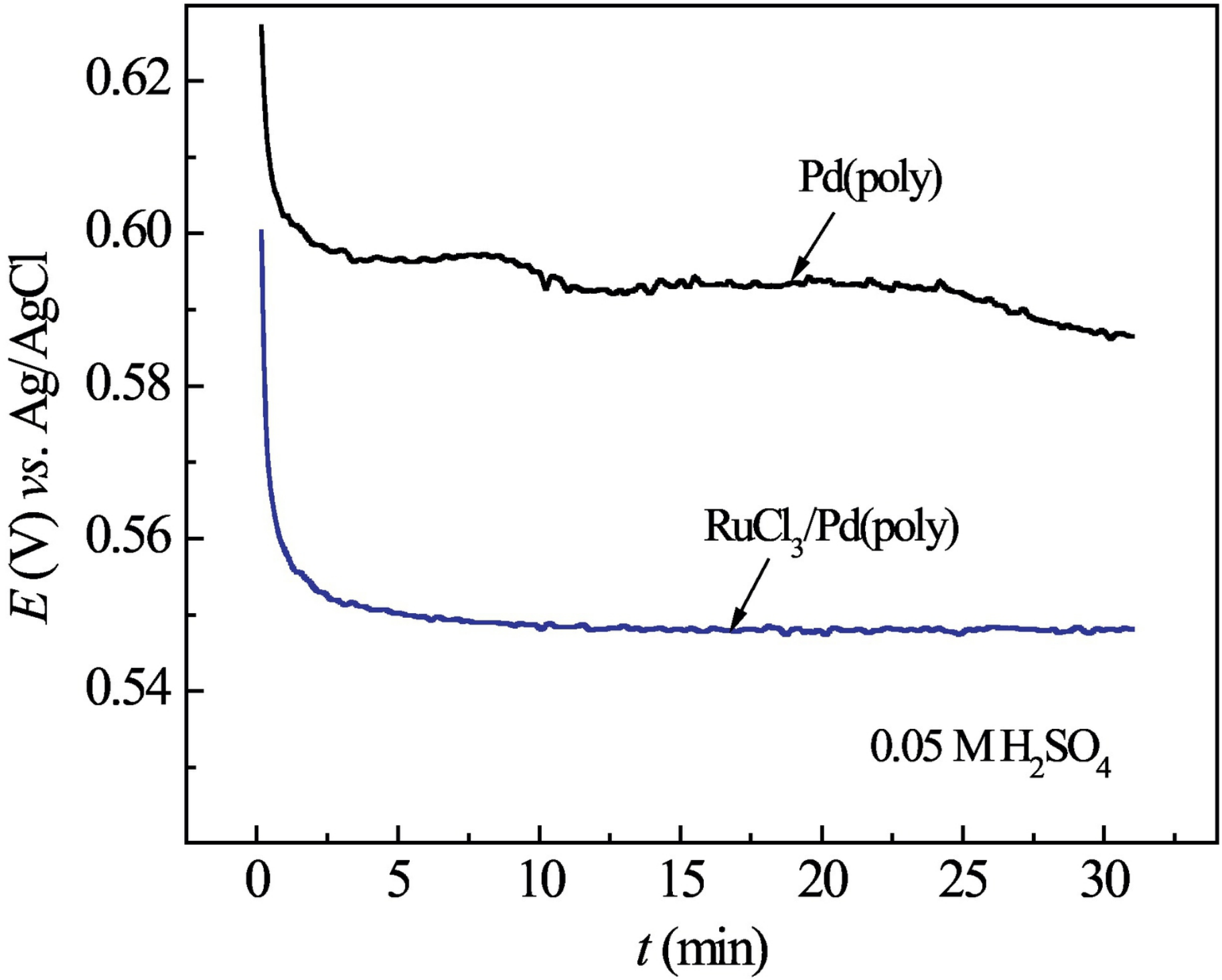
0.62
0.60
0.58
0.56
0.54
E (V) vs. Ag/AgCl
Pd(poly)
RuCl3/Pd(poly)
0.05 M H2SO4
0
5
10
15
20
25
30
t (min)

Figure 1

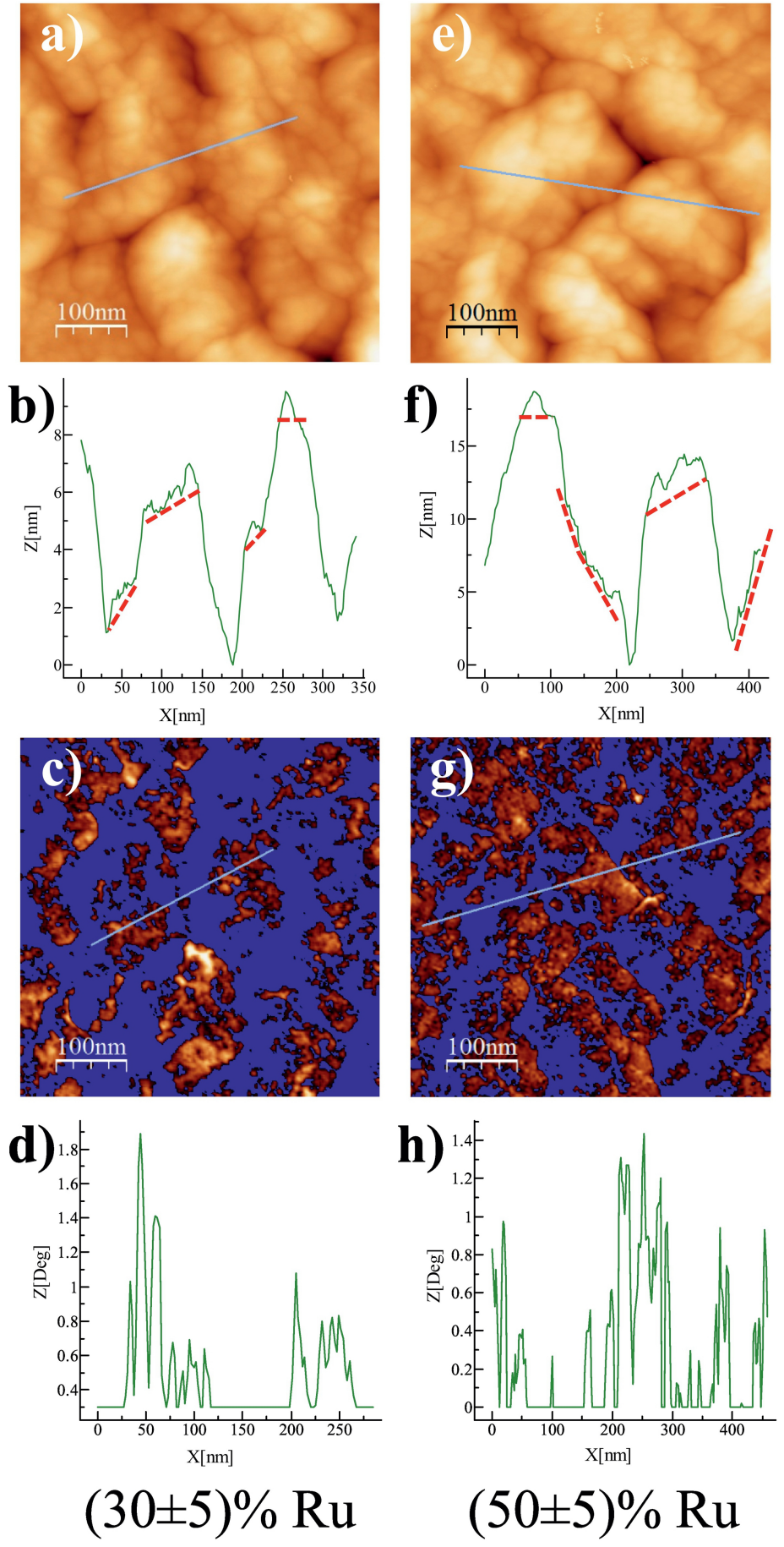
a)
100nm
e)
100nm
b)
Z[nm]
X[nm]
f)
Z[nm]
X[nm]
c)
100nm
g)
100nm
d)
Z[Deg]
X[nm]
h)
Z[Deg]
X[nm]
(30±5)% Ru
(50±5)% Ru

Figure 2

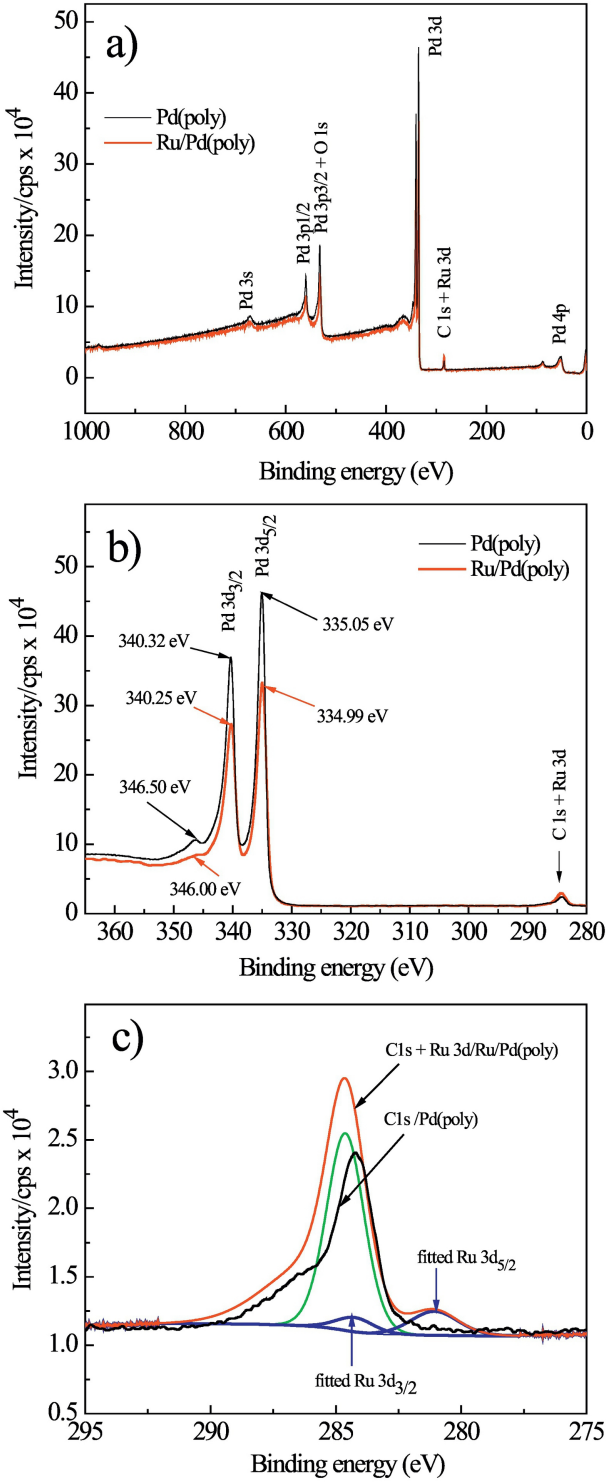
a)
Pd(poly)
Ru/Pd(poly)
Pd 3s
Pd 3p1/2
Pd 3p3/2 + O 1s
Pd 3d
C 1s + Ru 3d
Pd 4p
Intensity/cps x 10^4
Binding energy (eV)
b)
Pd(poly)
Ru/Pd(poly)
Pd 3d3/2
Pd 3d5/2
340.32 eV
340.25 eV
335.05 eV
334.99 eV
346.50 eV
346.00 eV
C 1s + Ru 3d
Intensity/cps x 10^4
Binding energy (eV)
c)
C1s + Ru 3d/Ru/Pd(poly)
C1s /Pd(poly)
fitted Ru 3d5/2
fitted Ru 3d3/2
Intensity/cps x 10^4
Binding energy (eV)

Figure 3

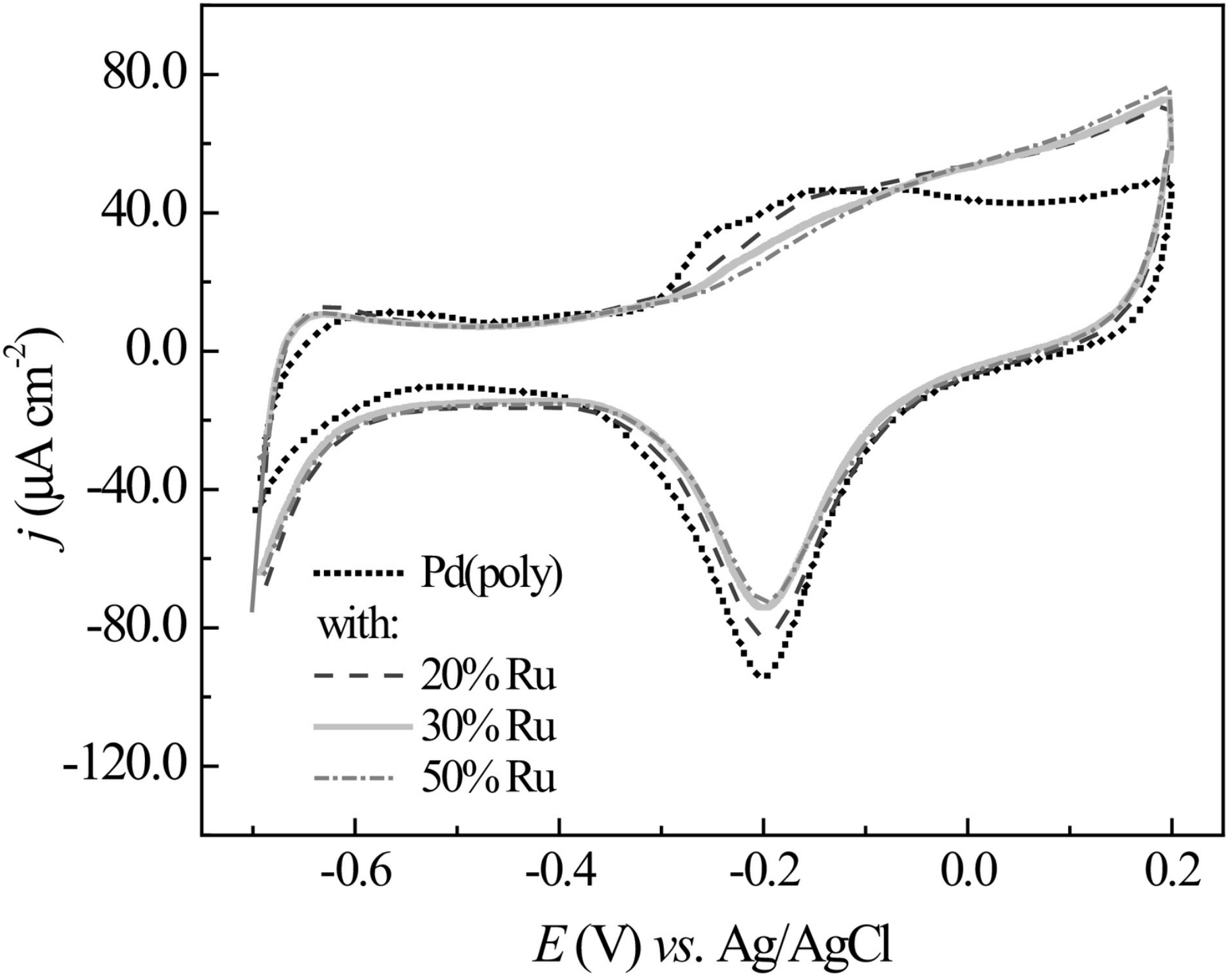
80.0
40.0
0.0
-40.0
-80.0
-120.0
j (μA cm-2)
Pd(poly)
with:
20% Ru
30% Ru
50% Ru
-0.6
-0.4
-0.2
0.0
0.2
E (V) vs. Ag/AgCl

Figure 4

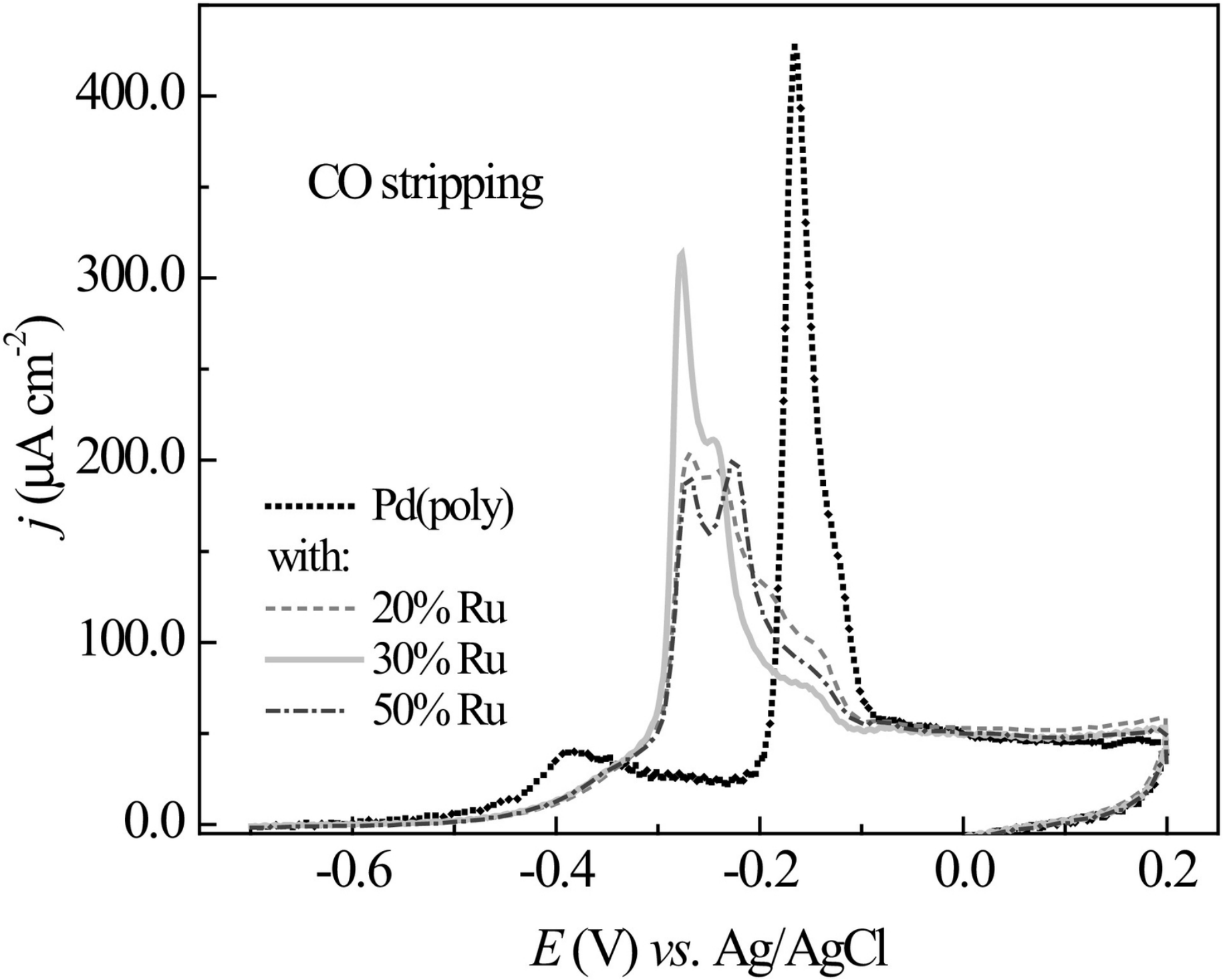
CO stripping
400.0
300.0
200.0
100.0
0.0
j (μA cm-2)
Pd(poly)
with:
20% Ru
30% Ru
50% Ru
-0.6
-0.4
-0.2
0.0
0.2
E (V) vs. Ag/AgCl

Figure 5

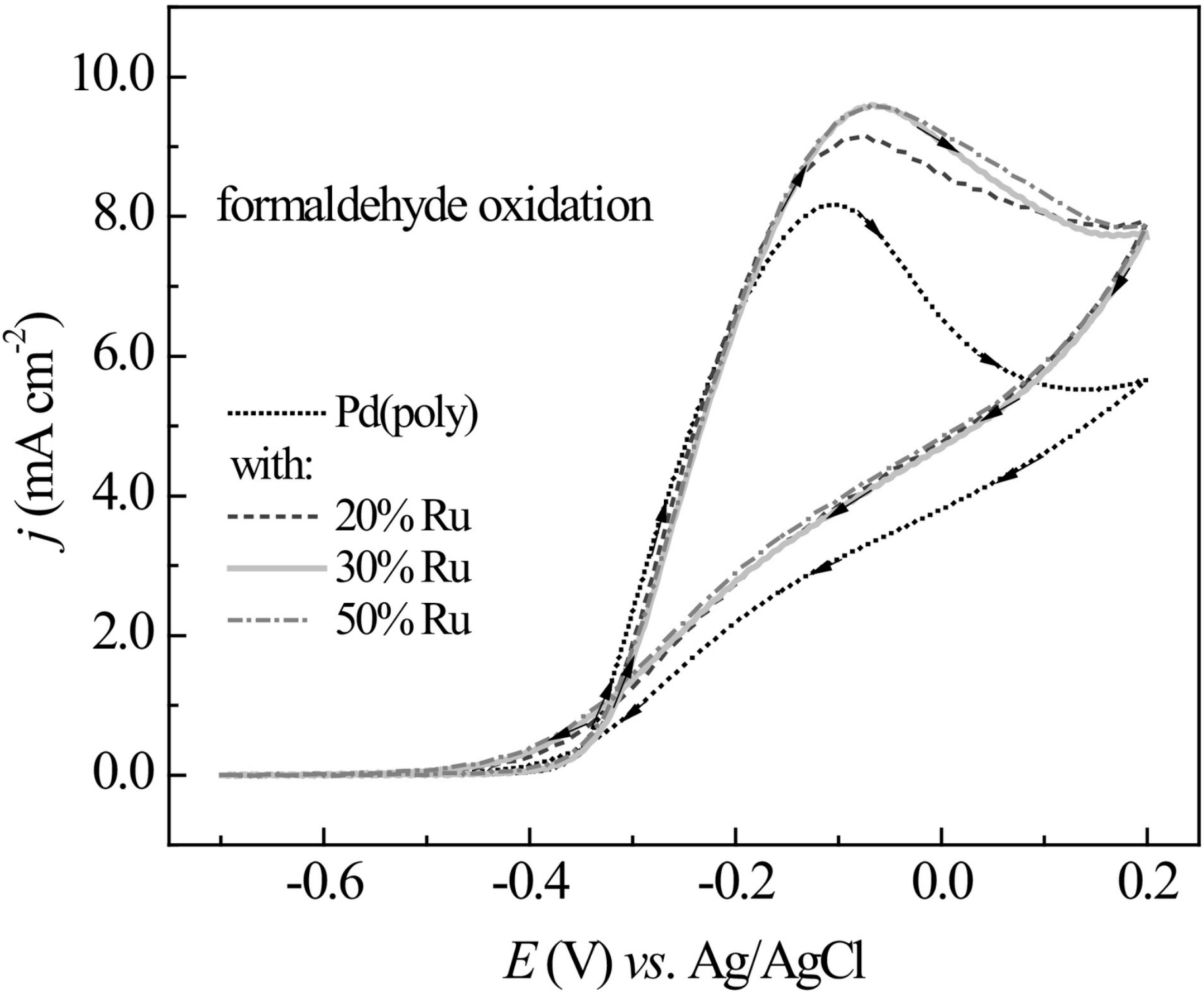
formaldehyde oxidation
Pd(poly)
with:
20% Ru
30% Ru
50% Ru
j (mA cm-2)
E (V) vs. Ag/AgCl
10.0
8.0
6.0
4.0
2.0
0.0
-0.6
-0.4
-0.2
0.0
0.2

Figure 6

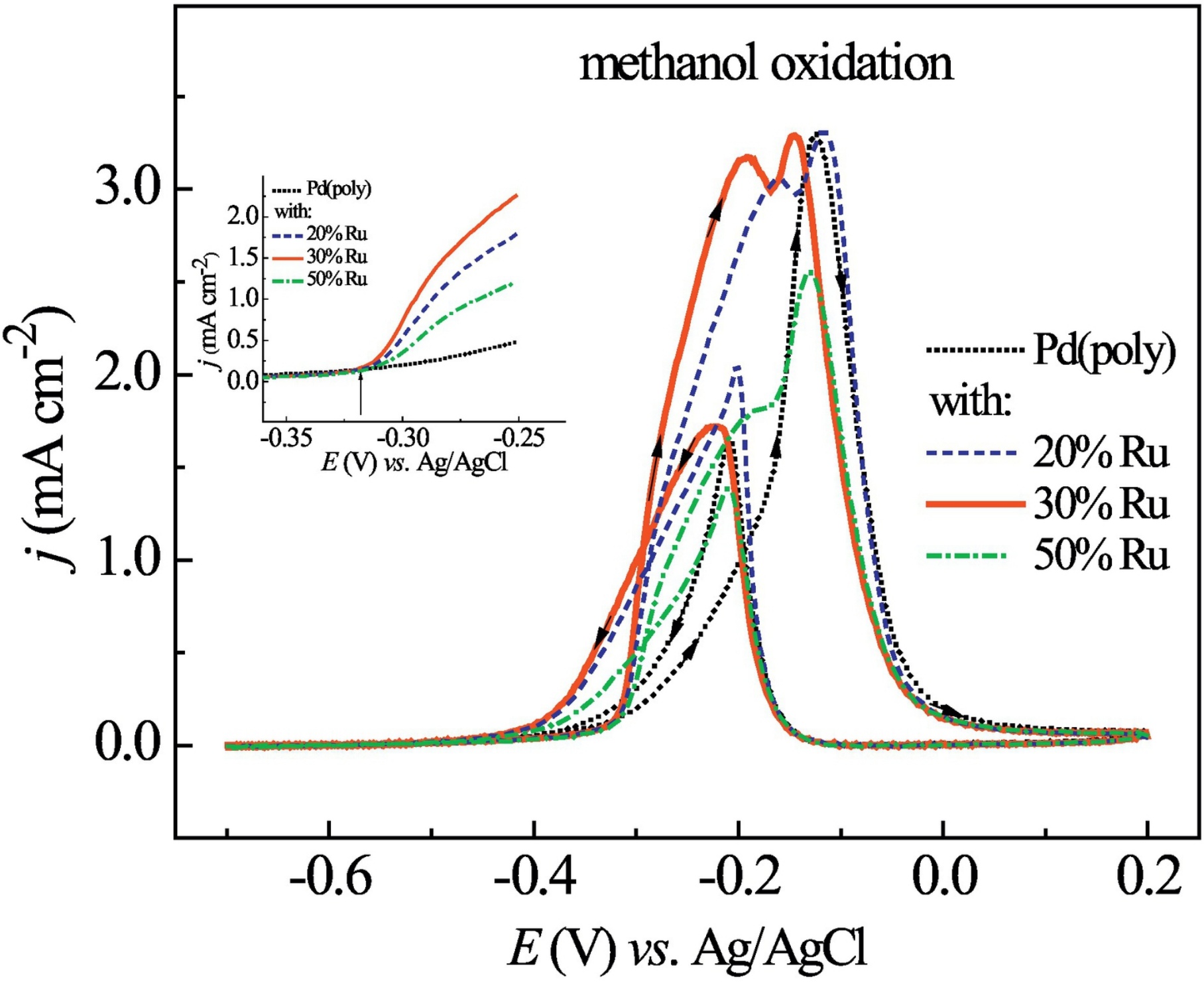
methanol oxidation
Pd(poly)
with:
20% Ru
30% Ru
50% Ru
j (mA cm-2)
E (V) vs. Ag/AgCl
3.0
2.0
1.0
0.0
-0.6
-0.4
-0.2
0.0
0.2
Pd(poly)
with:
20% Ru
30% Ru
50% Ru
j (mA cm-2)
2.0
1.5
1.0
0.5
0.0
-0.35
-0.30
-0.25
E (V) vs. Ag/AgCl

Figure 7

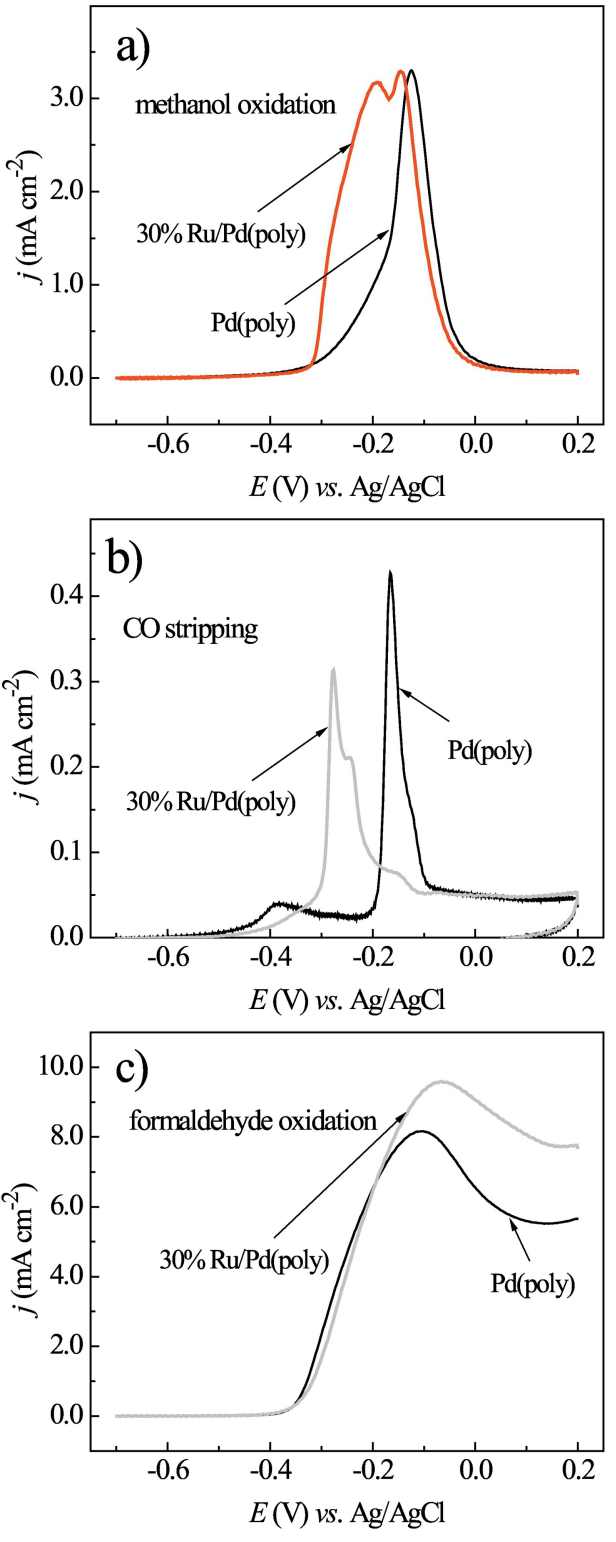
a)
methanol oxidation
30% Ru/Pd(poly)
Pd(poly)
j (mA cm-2)
E (V) vs. Ag/AgCl
b)
CO stripping
Pd(poly)
30% Ru/Pd(poly)
j (mA cm-2)
E (V) vs. Ag/AgCl
c)
formaldehyde oxidation
30% Ru/Pd(poly)
Pd(poly)
j (mA cm-2)
E (V) vs. Ag/AgCl

Figure 8

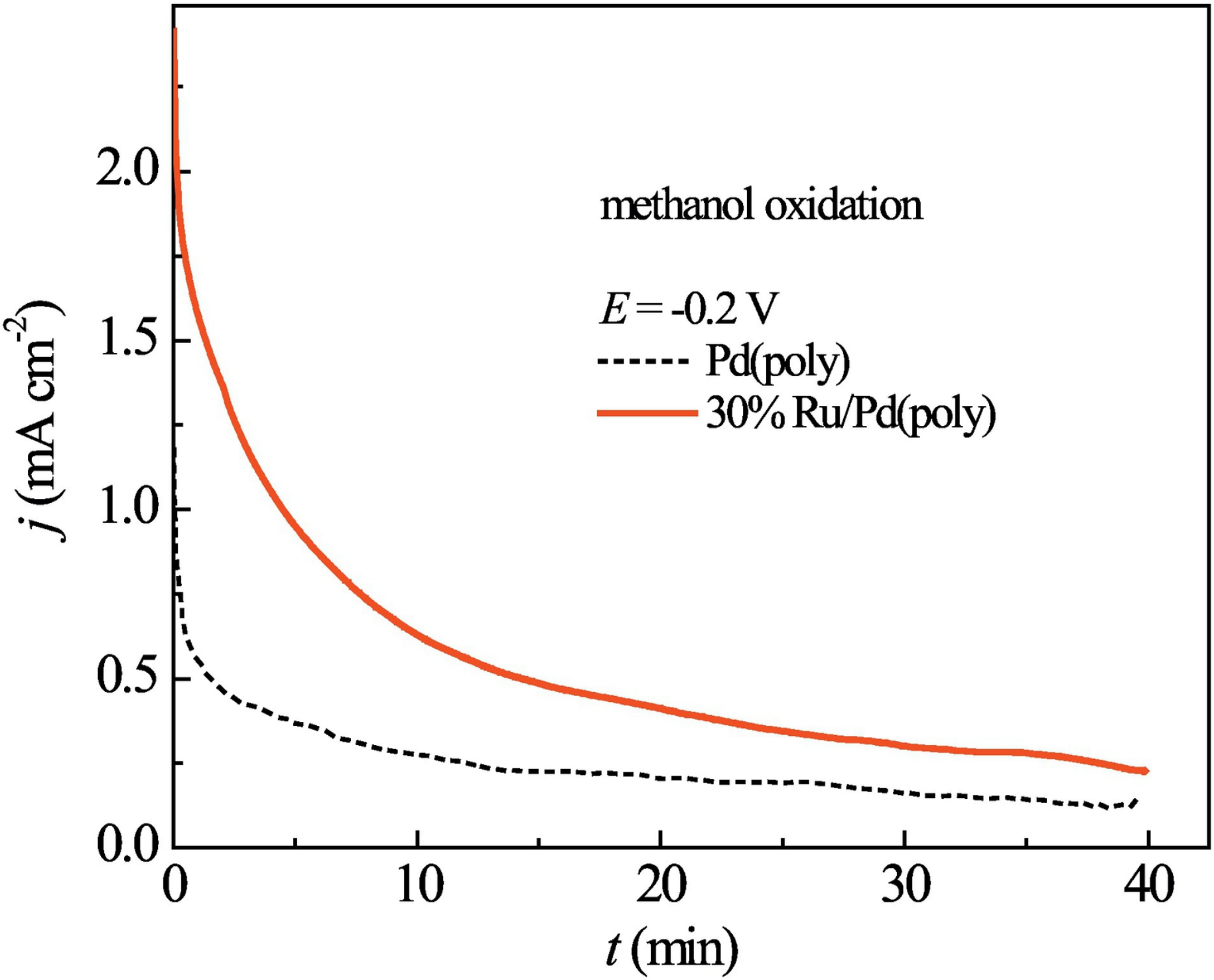
methanol oxidation
E = -0.2 V
Pd(poly)
30% Ru/Pd(poly)
j (mA cm-2)
t (min)
0.0
0.5
1.0
1.5
2.0
0
10
20
30
40

Figure 9